PROCEEDINGS OF SCIENCE

Rare and Semi-Rare Decays in ATLAS

Iskander Ibragimov*, **on behalf of the ATLAS collaboration**†
Department of Physics, University of Siegen, Walter-Flex-Str. 3, 57068 Siegen, Germany
E-mail: ibragimov@hep.physik.uni-siegen.de

Flavour-changing neutral-current processes like $b \to s\mu^+\mu^-$ and $B^0_{(s)} \to \mu^+\mu^-$ are suppressed in the Standard Model and thus sensitive to New Physics effects. This contribution summarises ATLAS results from the angular analysis of the $B^0 \to K^*\mu^+\mu^-$ decay performed with LHC Run 1 data, the $\mathscr{B}(B^0_{(s)} \to \mu^+\mu^-)$ measurement performed with 2015 and 2016 data and projections for the $B^0 \to K^*\mu^+\mu^-$ and $\mathscr{B}(B^0_{(s)} \to \mu^+\mu^-)$ measurements for the High-Luminosity LHC (HL-LHC). The projections are based on extrapolations of the Run 1 results with the expected statistics corresponding to an assumed 3 ab^{-1} of delivered luminosity for the HL-LHC and on simulations of the expected layout of a new Inner Tracker.

European Physical Society Conference on High Energy Physics - EPS-HEP2019 -
10-17 July, 2019
Ghent, Belgium

*Speaker.

†This work was supported in part by grants of the German Federal Ministry of Education and Research (BMBF).

PoS(EPS-HEP2019)241

1. Analysis of $B^0 \to K^*\mu^+\mu^-$: current status and prospects at the HL-LHC

The decay $B^0 \to K^*\mu^+\mu^-$, where $K^* \to K^+\pi^-$, can proceed in the SM only via loop diagrams, mediated by flavour-changing neutral currents (FCNC). The angular structure of this decay is complex and can be fully described by three angles and the dimuon invariant mass squared q^2. Multiple angular observables provided by this decay can be sensitive to different types of New Physics (NP). The LHCb collaboration reported a 3.4σ deviation from the Standard Model (SM) calculations [1]. Therefore the ATLAS measurement [2], performed using 20.3 fb^{-1} of pp collision data at a centre-of-mass energy $\sqrt{s} = 8$ TeV collected in 2012, adopts the LHCb methodology, definitions of angular observables and of optimised parameters $P_i^{(')}$[3]. The latter are designed to minimise uncertainties from hadronic form factors and thus increase sensitivity to NP. Due to limited statistics a set of trigonometric transformations of angular variables [3] is employed in our analysis. A description of the ATLAS detector can be found in [4].

Data are combined from 19 trigger chains with one, two, or at least three identified muons in order to maximise the signal yield and to ensure analysis sensitivity down to the kinematic threshold of $q^2 = 0.04$ GeV^2. Signal candidates are reconstructed from two charged tracks satisfying $K\pi$ mass hypothesis and a pair of oppositely charged muons. Cut-based selections on vertex fit quality, B^0 lifetime significance τ/σ_τ, pointing angle and $p_{\mathrm{T}}(K^*)$ are used to suppress the combinatorial background. The selected data sample consists of 787 events in the signal q^2 range of [0.04, 6.0] GeV^2. Data with q^2 above 6 GeV^2 are not studied since background significantly increases due to a radiative tail from $B^0 \to K^*J/\psi$ events.

An extended unbinned maximum-likelihood fit of the angular distribution of the decay is performed in order to extract the angular parameters in six bins of q^2, with three of these bins overlapping. A total of 342 ± 39 signal events is found by the fit. Two distinct background contributions from partially reconstructed $B \to D^0/D^+_{(s)}X$ and $B^+ \to K^+/\pi^+\mu^+\mu^-$ decays are observed peaking in the distributions of angular variables in data. By excluding the affected part of the distributions or the events around B^+ and $D^0/D^+_{(s)}$ masses from the fit systematic uncertainties are assigned. The largest systematic uncertainty comes from fake K^* candidates. Overall, the statistical uncertainty largely dominates.

In Figure 1 the results for the $P_4^{'}$ and $P_5^{'}$ parameters are compared to the theoretical computations of Jäger and Camalich (JC) [5], Descotes-Genon et al. (DHMV) [6] and Ciuchini et al. (CFFMPSV) [7]; the results from LHCb [1], Belle [8] and CMS [9] are also overlaid. The $P_4^{'}$ and $P_5^{'}$ measurements in the $q^2 \in [4.0, 6.0]$ GeV^2 bin are observed to be $\sim 2.7\sigma$ away from the DHMV model. The LHCb collaboration observed a similar deviation for $P_5^{'}$ [1]. Overall, all ATLAS measurements are within three standard deviations of the different theoretical expectations and also compatible with the results of the other experiments.

The Run 1 result is used as a baseline for HL-LHC projections of the analysis. Accounting for a $\times 1.7$ increase in the b production cross-section and considering three potential trigger scenarios, multiples of 50 ("conservative"), 160 ("intermediate") and 250 ("high yield") of the Run 1 statistics are obtained. It is also expected that with a new all-silicon Inner Tracker (ITk) the resolution in the reconstructed 4-prong invariant mass will improve by 30%. To estimate the achievable experimenal precision, pseudo-MC experiments based on Run 1 signal and background angular distributions are performed. The same fitting procedure as in the Run 1 analysis is employed.

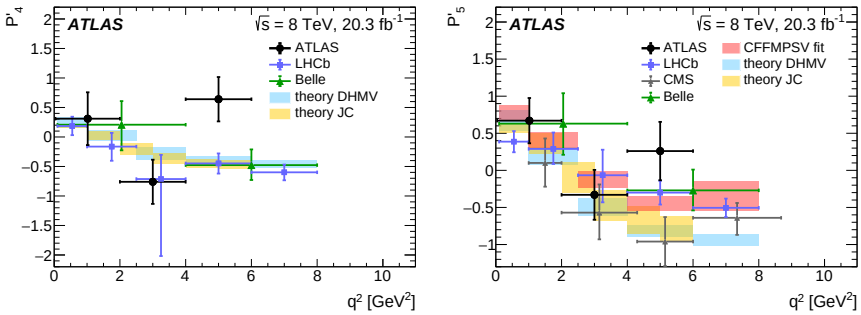

Figure 1 – The measured values of $P_4^{'}$ (left) and $P_5^{'}$ (right) parameters compared with other experimental results and predictions from theoretical calculations [2].

Assuming that the increased statistics will allow for a better fit model and for a better knowledge of exclusive backgrounds, the corresponding systematic uncertainties are scaled by $1/\sqrt{L_{\text{int}}}$. Figure 2 demonstrates the expected improvement in the accuracy of the $P_4^{'}$ and $P_5^{'}$ parameters compared to the current theoretical predictions. Quantitatively, the precision in measuring the $P_5^{'}$ parameter is expected to improve by a factor of 5, 8 or 9 relative to the Run 1 measurement depending on the trigger scenario, as described above.

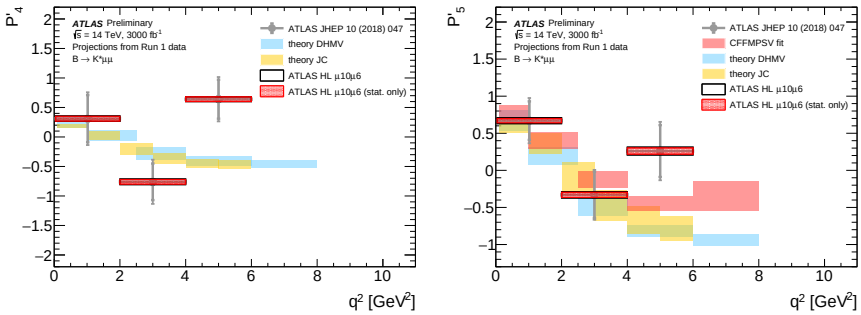

Figure 2 – Projected statistical (hatched regions) and total (open box) uncertainties on the $P_4^{'}$ (left) and $P_5^{'}$ (right) parameters against q^2 for the intermediate $\mu 10\mu 6$ trigger scenario at HL-LHC compared to predictions from theoretical calculations and the ATLAS Run 1 measurement. The statistical and total uncertainties of the latter are shown by inner and outer vertical bars, respectively. While the HL-LHC toy-MC were generated with the DHMV central values of the $P_4^{'}$ and $P_5^{'}$ parameters, in these plots the central values are moved to the ATLAS Run 1 measurement for better visualisation of the improvement in the precision [10].

2. $B^0_{(s)} \to \mu^+\mu^-$ measurement: current status and prospects at the HL-LHC

The rare $B^0_s \to \mu^+\mu^-$ decay and even more rare $B^0 \to \mu^+\mu^-$ decay are FCNC processes, which are very strongly suppressed in the SM, with accurately predicted branching fractions of $\mathscr{B}(B^0_s \to \mu^+\mu^-) = (3.65 \pm 0.23) \times 10^{-9}$ and $\mathscr{B}(B^0 \to \mu^+\mu^-) = (1.06 \pm 0.09) \times 10^{-10}$ [11]. The ATLAS Run 1 result [12] is compatible with the SM at the $\sim 2\sigma$ level and the $\mathscr{B}(B^0_{(s)} \to \mu^+\mu^-)$ values are lower than the CMS-LHCb combined result [13]. A more recent LHCb update [14] with

part of the Run 2 data sets an upper limit of $\mathscr{B}(B^0 \to \mu^+\mu^-) < 3.4 \times 10^{-10}$ at 95% confidence level (CL), which reduces the tension in this observable.

The updated ATLAS measurement [15] is performed using 36.2 fb^{-1} of LHC Run 2 data taken at a centre-of-mass energy of 13 TeV during 2015 and 2016. Events are selected by a single dimuon trigger, requiring one muon with $p_{\mathrm{T}} > 4$ GeV and the other with $p_{\mathrm{T}} > 6$ GeV as well as the dimuon invariant mass $m_{\mu\mu}$ in the range of 4 GeV to 8.5 GeV. Much stricter selections are applied offline - in particular, the analysis employs a 15-variable Boosted Decision Tree (BDT) in the final selection to suppress the dominant background contribution from the combinatorial $b\bar{b} \to \mu^+\mu^- X$ events. The BDT is trained and tested using simulated signal events and events from data sidebands. A 360-MeV-wide signal region starting at 5166 MeV remained blinded until the procedures for event selection and signal yield extraction were fully defined. The left mass sideband contains partially reconstructed decays like $b \to \mu^+\mu^- X$ (e.g. $b \to c\mu X \to s(d)\mu^+\mu^- X$ cascades and B-decays to dimuons $B \to \mu^+\mu^- X$), as well as $B_c \to J/\psi\mu\nu$ and semi-leptonic $B^0_{(s)}/\Lambda^0_b \to h\mu\nu$ decays. High-mass tails of these backgrounds reach signal region and are taken into account in the signal fit. A peaking background due to $B^0_{(s)} \to hh'$, with misidentification of hh' as $\mu^+\mu^-$, yields 2.9 ± 2.0 events in the signal region after *tight* muon selections. As for the normalisation channel, an abundant decay $B^+ \to J/\psi(\to \mu^+\mu^-)K^+$, with a well-measured branching fraction, is used. It is also employed for kinematic corrections of simulated signal events as well as for validation of BDT input variables by comparisons of data and simulation.

$B^0_{(s)}$ signal events are extracted by using an unbinned maximum likelihood fit to the dimuon mass distributions in four BDT bins. The fit, shown in Figure 3a for the most sensitive BDT bin, returns $N_s = 80 \pm 22$ of $B^0_s \to \mu^+\mu^-$ and $N_d = -12 \pm 20$ of $B^0 \to \mu^+\mu^-$ events, which is consistent with the SM expectations of $N_s^{SM} = 91$ and $N_d^{SM} = 10$, respectively. The same fit has been repeated, replacing the fit parameters N_s and N_d by the corresponding branching fractions divided by normalisation terms and including uncertainties of the latter. A Neyman construction [16] is used to determine the 68.3% confidence interval for $\mathscr{B}(B^0_s \to \mu^+\mu^-)$ and to set an upper limit on $\mathscr{B}(B^0 \to \mu^+\mu^-)$. The results are $\mathscr{B}(B^0_s \to \mu^+\mu^-) = \left(3.21^{+0.96}_{-0.91}(\mathrm{stat.})^{+0.49}_{-0.30}(\mathrm{syst.})\right) \times 10^{-9}$ and $\mathscr{B}(B^0 \to \mu^+\mu^-) < 4.3 \times 10^{-10}$ at 95% CL, respectively. The likelihood function of the measurement is combined with that of Run 1 as shown in Figure 3b with the help of contours, obtaining $\mathscr{B}(B^0_s \to \mu^+\mu^-) = \left(2.8^{+0.8}_{-0.7}\right) \times 10^{-9}$ and $\mathscr{B}(B^0 \to \mu^+\mu^-) < 2.1 \times 10^{-10}$ at 95% CL. The combination yields a combined significance of the $B^0_s \to \mu^+\mu^-$ signal of 4.6σ and is compatible with the SM at the level of 2.4σ.

At the HL-LHC, apart from the increased statistics, the BR($B^0_{(s)} \to \mu^+\mu^-$) measurement will greatly benefit from the improved $B^0_{(s)}$ invariant mass resolution, which will allow for a better separation of B^0_s and B^0 signals. A study [17] shows that the separation of the B^0_s and B^0 mass peaks will be improved by a factor of 1.65 (1.5) to 2.3σ (1.3σ) in the barrel (end-cap) region compared to Run 1, mainly due to the lower material budget of the ITk. Using this result and pseudo-experiments based on the likelihood of the Run 1 analysis, another study [18] investigated the potential for measuring $\mathscr{B}(B^0_{(s)} \to \mu^+\mu^-)$ with the expected datasets from the HL-LHC (3 ab^{-1}). Taking into account the prescales of topological dimuon triggers, three potential trigger scenarios are considered, yielding multiples of 15 ("conservative"), 60 ("intermediate") and 70 ("high yield") of the Run 1 statistics. The internal sources of systematic uncertainties, such as

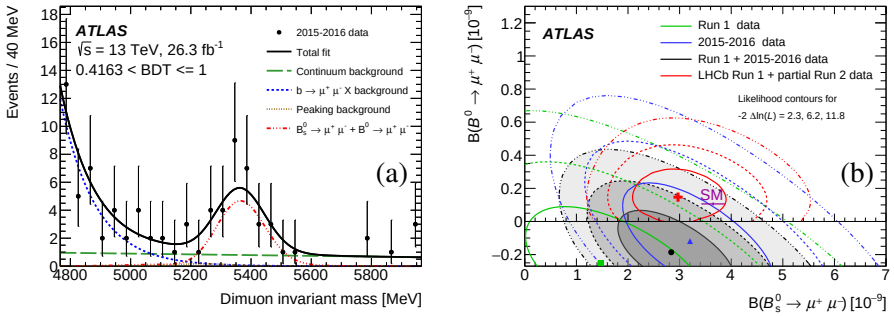

Figure 3 – *(a)* Dimuon invariant mass distribution in the unblinded data, in the BDT interval with the highest signal-to-background ratio. The result of the maximum-likelihood fit is overlaid. The total fit is shown as a continuous line, with the dashed lines corresponding to the observed signal component, the $b \to \mu\mu X$ background, and the continuum background. The signal components are combined into one single curve, including both the $B_s^0 \to \mu^+\mu^-$ and the (negative) $B^0 \to \mu^+\mu^-$ component. The curve representing the peaking $B^0_{(s)} \to hh'$ background lies very close to the horizontal axis. *(b)* Likelihood contours for the combination of the Run 1 and 2015−2016 Run 2 results (shaded areas). The contours are obtained by combination of the two analyses' likelihoods, for values of $-2\Delta\ln(\mathscr{L})$ equal to 2.3, 6.2 and 11.8. The contours for the individual Run 2 2015−2016 and Run 1 results as well as the ones from the latest LHCb result [14] are overlaid. The SM predictions and their uncertainties [11] are included. Figures taken from [15].

those on the fit shapes and efficiencies, were scaled according to the increase in statistics whereas the external ones, such as those on the $\mathscr{B}(B^\pm \to J/\psi K^\pm)$ and the b-quark fragmentation fractions $f_s/f_{d(u)}$, were conservatively kept the same as in the Run 1 analysis. The latter contribution dominates the systematic uncertainty on $\mathscr{B}(B_s^0 \to \mu^+\mu^-)$. The contours in Figure 4 demonstrate the expected improvement in the accuracy of the $\mathscr{B}(B^0_{(s)} \to \mu^+\mu^-)$ measurements at the HL-LHC.

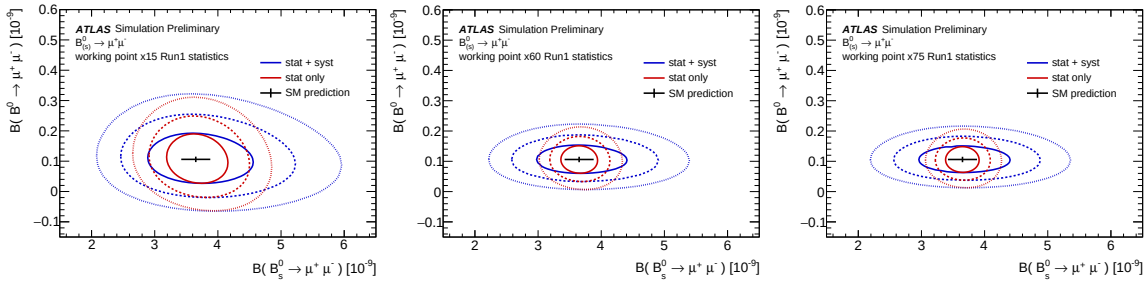

Figure 4 – Contours of 68.3% (solid), 95.5% (dashed) and 99.7% (dotted) confidence levels for (from left to right) the "conservative", "intermediate" and "high yield" HL-LHC extrapolation scenarios [18], obtained using a profiled likelihood. Red contours are statistical only; blue contours include systematic uncertainties extrapolated from the Run 1 analysis. The black points show the SM theoretical prediction and its uncertainty [11].

3. Summary

Measurements of rare and semi-rare FCNC decays sensitive to new physics contributions were performed by the ATLAS collaboration at the LHC. The results of the angular analysis of the

$B^0 \to K^* \mu^+ \mu^-$ decay with 20.3 fb^{-1} of Run 1 data agree with the theoretical predictions in the SM and other measurements, with the largest deviation of $\sim 2.7\sigma$ from theory observed for the $P_4^{'}$ and $P_5^{'}$ parameters in the $q^2 \in [4.0, 6.0]$ GeV^2 bin. The measurement of $\mathscr{B}(B_s^0 \to \mu^+\mu^-)$ and the search for the decay $B^0 \to \mu^+\mu^-$ with 36.2 fb^{-1} of 2015 and 2016 data, combined with the ATLAS Run 1 result, agree with the SM and other experimental results. The ATLAS measurement sets an upper limit of $\mathscr{B}(B^0 \to \mu^+\mu^-) < 2.1 \times 10^{-10}$ at 95% CL, which is the most stringent to date. The sensitivity of both analyses will benefit from the increased statistics expected from the 3 ab^{-1} of HL-LHC data as well as from the better mass resolution expected due to the new Inner Tracker. This will improve discovery potential for physics beyond the SM.

References

[1] LHCb Collaboration, *Angular analysis of the $B^0 \to K^{*0}\mu^+\mu^-$ decay using 3 fb^{-1} of integrated luminosity*, JHEP **02** (2016) 104, arXiv: 1512.04442 [hep-ex].

[2] ATLAS Collaboration, *Angular analysis of $B_d^0 \to K^*\mu^+\mu^-$ decays in pp collisions at $\sqrt{s} = 8$ TeV with the ATLAS detector*, JHEP **10** (2018) 47, arXiv: 1805.04000 [hep-ex].

[3] LHCb Collaboration, *Measurement of Form-Factor Independent Observables in the Decay $B^0 \to K^{*0}\mu^+\mu^-$*, Phys. Rev. Lett. **111** (2013) 191801, arXiv: 1308.1707 [hep-ex].

[4] ATLAS Collaboration, *The ATLAS Experiment at the CERN Large Hadron Collider*, JINST **3** (2008) S08003.

[5] S. Jäger and J. Martin Camalich, *Reassessing the discovery potential of the $B \to K^*\ell^+\ell^-$ decays in the large-recoil region: SM challenges and BSM opportunities*, Phys. Rev. D **93** (2016) 014028, arXiv: 1412.3183 [hep-ph].

[6] S. Descotes-Genon et al., *On the impact of power corrections in the prediction of $B \to K^*\mu^+\mu^-$ observables*, JHEP **12** (2014) 125, arXiv: 1407.8526 [hep-ph].

[7] M. Ciuchini et al., *$B \to K^*\ell^+\ell^-$ decays at large recoil in the Standard Model: a theoretical reappraisal*, JHEP **06** (2016) 116, arXiv: 1512.07157 [hep-ph].

[8] Belle Collaboration, *Measurement of the Differential Branching Fraction and Forward-Backward Asymmetry for $B \to K^{(*)}l^+l^-$*, Phys. Rev. Lett. **103** (2009) 171801, arXiv: 0904.0770 [hep-ex].

[9] CMS Collaboration, *Angular analysis of the decay $B^0 \to K^{*0}\mu\mu$ from pp collisions at $\sqrt{s}$ = 8 TeV*, Phys. Lett. B **753** (2016) 424, arXiv: 1507.08126 [hep-ex].

[10] ATLAS Collaboration, *$B_d^0 \to K^*\mu^+\mu^-$ angular analysis prospects with the upgraded ATLAS detector at the HL-LHC*, ATL-PHYS-PUB-2019-003.

[11] C. Bobeth et al., *$B_{(s)}^0 \to \ell^+\ell^-$ in the Standard Model with Reduced Theoretical Uncertainty*, Phys. Rev. Lett. **112** (2014) 101801, arXiv: 1311.0903 [hep-ph].

[12] ATLAS Collaboration, *Study of the rare decays of B_s^0 and B^0 into muon pairs from data collected during the LHC Run1 with the ATLAS detector*, Eur. Phys. J. C (2016) 76:513, arXiv: 1604.04263 [hep-ex].

[13] CMS and LHCb Collaborations, *Observation of the rare $B_s^0 \to \mu^+\mu^-$ decay from the combined analysis of CMS and LHCb data*, Nature, **522**, 2015.

[14] LHCb Collaboration, *Measurement of the $B_s^0 \to \mu^+\mu^-$ branching fraction and effective lifetime and search for $B^0 \to \mu^+\mu^-$ decays*, Phys. Rev. Lett. **118** (2017) 191801, arXiv: 1703.05747 [hep-ex].

[15] ATLAS Collaboration, *Study of the rare decays of B_s^0 and B^0 into muon pairs using data collected during 2015 and 2016 with the ATLAS detector*, JHEP **04** (2019) 098, arXiv: 1812.03017 [hep-ex].

[16] J. Neyman, *Outline of a Theory of Statistical Estimation Based on the Classical Theory of Probability*, Phil. Trans. R. Soc. London A, **236** (1937) 333-380.

[17] ATLAS Collaboration, *Expected performance for an upgraded ATLAS detector at High-Luminosity LHC*, ATL-PHYS-PUB-2016-026.

[18] ATLAS Collaboration, *Prospects for the $\mathscr{B}(B^0_{(s)} \to \mu^+\mu^-)$ measurements with the ATLAS detector in Run 2 LHC and HL-LHC data campaigns*, ATL-PHYS-PUB-2018-005.